行政院國家科學委員會補助專題研究計畫成果報告

※※※※※※※※※※※※※※※※※※※※※※※

※ 坩鍋旋轉對單晶生長製成之熱質流影響及控制 ※

※※※※※※※※※※※※※※※※※※※※※※※

計畫類別：■個別型計畫 □整合型計畫

計畫編號：NSC 89－2214－E－002－040

90-2214-E-002-015

執行期間：2000年 8月 1日至 2002年 7月 31日

計畫主持人：藍崇文 教授

本成果報告包括以下應繳交之附件：

□赴國外出差或研習心得報告一份

□赴大陸地區出差或研習心得報告一份

☒出席國際學術會議心得報告及發表之論文各一份

□國際合作研究計畫國外研究報告書一份

中 華 民 國 91年 10月

行政院國家科學委員會專題研究計畫成果報告
Segregation and Morphological Instability due to Double-Diffusive Convection in Rotational Directional Solidification

計劃編號：89-2214-E-002-040
執行期限: 2000 年 8 月 1 日至 2002 年 7 月 31 日

主持人:藍崇文教授 [1]
計畫參與人員:楊雅雯、陳煌仁、李逸飛
[1]Department of Chemical Engineering, National Taiwan University, Taipei, Taiwan 10617, ROC

Abstract –Through computer simulation and direct observation of the freezing interface during directional solidification of succinonotrile containing acetone on a rotating table, the effect of double-diffusive flows due to gravitational and centrifugal forces on solute transport and morphological instability is investigated. Without rotation, the concave interface due to solidification induced buoyant convection and resulted in local solute accumulation at the center of the interface. This led to pit formation and accelerated morphological breakdown. At medium rotation rate, the convection near the interface was suppressed, but the fast buildup of the solute caused much larger interface deformation and earlier morphological breakdown. However, if the rotation rate was high enough, the flow direction near the interface could be reversed and solute accumulation slowed down. Pit formation was eliminated as well.

Keywords: crystal growth, rotational directional solidification, segregation

Introduction

In this report, we present the observation of the freezing interface during directional solidification of SCN containing acetone on a rotating table. As will be shown, rotation strongly affects the solute transport, both radial and axial, with changes in interface morphology clearly revealing the effects of rotation. Morphological instability during solidification at various conditions is also discussed. A computer simulation is also presented to better understand the key transport mechanisms. In the next section, the material purification and experimental setup are described. The results are also presented later, followed by the conclusion.

Experimental

Succinonitrile (SCN) was directionally solidified using a transparent vertical Bridgman system(higher than 99.999wt%[4]). To consider the solutal effect, a small amount of acetone (0.007wt%) was injected into the sample through a 5μl micro-syringe inserted into the bottom of the sample. We have also used ethanol as a solute [5]. The Bridgman furnace consisted of two heating zones made of copper blocks each with a nichrome wire inside as a heating element. The whole solidification system was installed on a rotating table (80cm in diameter), as shown in Fig.1. The ampoule position was carefully adjusted by a He/Ne laser beam during rotation, so that the rotation axis is aligned as much as possible with the ampoule axis.

An axisymmetric numerical model accounting for melt convection, heat and mass transfer, and the moving interface [6-7] was used to simulate the solidification and to better understand the observed phenomena.

$$d_\omega = \Pr\left(Ra_T\left(\frac{\partial T}{\partial r} + rFr\frac{\partial T}{\partial z}\right) + Ra_S\left(\frac{\partial C}{\partial r} + rFr\frac{\partial C}{\partial z}\right)\right) - \Pr Ta^{1/2}\frac{\partial v_\theta}{\partial z} \quad (2)$$

An efficient finite-volume/Newton's method was used to solve the field variables and the interface simultaneously. In the simulation, the heating profile is described

by a hyperbolic tangent function fitting to the measured one. Detailed numerical implementation and parameter study will be discussed elsewhere [24]. In addition, during calculation, the thermal (G_T) and solutal (G_S/m) gradients at the interface, where m is the slope of the liqudus-temperature line, also provide important information for morphological instability due to constitutional supercooling. The criterion proposed by Mullins and Sekerka [1] is used:

$$G_T - G_S d < 0. \qquad (3)$$

In the above equation, d is a parameter related to interfacial energy. For SCN, this value is about unity. Therefore, the interface becomes unstable as soon as the constitutional supercooling exists.

Results

Fig. 2 shows a sequence of interface evolution at 2μm/s for the purified sample; simulated results (stream lines as on the left and isotherms on the right) are also put together for comparison. After the interface concavity develops, there are two flow cells in the melt. This two-cell flow structure is typical for the Bridgman configuration [8]. The lower cell is due to the interface concavity and the upper cell is due to the mismatch condition between the adiabatic and hot zones.

With 0.007wt% acetone at the growth rate of 2.5μm/s as shown in Fig. 3, after one hour (3b), a clear pit formed at the interface center. The morphology started to breakdown from the pit tip at about 90 min (3c). Since then, the broken down area spread out slowly with time as the one shown in Fig. 3d; the newly solidified material behind became less transparent. This interface breakdown through pit formation is quite similar to the one observed by Schaefer and Coriell [1], where ethanol was used as the solute. The significant buildup of the solute near pit formation (3b) and the onset of supercooling (3c) is also clear. As discussed by Lan and Tu [4], the overall flow is dominated by thermal convection. The solutal effect mainly influences the pit shape and the onset of constitutional supercooling. With a lower growth rate at 2μm/s, the observed interface evolution was similar, but no interface breakdown was observed in 3 hours.

With 100 RPM rotation, the interface evolution is shown in Fig. 4. As shown, before the growth was started, the interface was slightly concave. The interface broke down at about 6207s (4d), while no instability was observed in 3 hours for no rotation. The pit shapes were also very different, as shown in Fig. 4d, a cusp tip appeared. The earlier morphological instability and the more significant interface deformation are believed to be more solute accumulation in front of the interface. Indeed, as discussed by Lan and Tu [3], before the magic-g level, the convection is suppressed by rotation. Especially, the cusp interface shape was predicted. The calculated onset of supercooling also agrees well with the observed one being about at 6000s as well. One can also compare the maximum solute content (C_{max}/C_0) with the previous cases showing the faster solute buildup during rotation.

Increasing the rotation rate to 150RPM, as shown in Fig. 5, let to a very different interface shape with no pit formation at the interface center. Instead, the interface shape involved a transition from a flat bottom to a sloped edge. As will be shown shortly, this transition is due to the local solute accumulation. Due to the much weaker flow near the interface, the solutal field there becomes very diffusive. Nevertheless, the buildup rate of the concentration decreased significantly as compared C_{max}/C_0 with that in Fig. 4. This is simply due to the rim (larger r) of the interface having a larger area, as compared with the interface center (small r), to accommodate the solute rejected from the interface during solidification.

To get a stable growth front, 200 RPM was required. Fig. 6 shows the effects of rotation rate on the interface morphology after 3 hours of growth. From the

breakdown patterns of the interface, one can easily figure out the distribution of solute accumulation. The calculated result for 200 RPM is put together for comparison. As shown in Fig. 6d, the inward flow cell near the interface is removed. As a result, the solute accumulates near the rim of the interface. Fig. 7 summarizes the double-diffusive flows due to both gravity and rotation. Without rotation (Fig. 7a), the thermal and solutal flows near the interface are in the same direction; both are inward; the gravitational acceleration is pointing downwards. With rotation, the axial density gradient being perpendicular to the centrifugal acceleration can induce flow. Because the lighter solute accumulates near the interface, the affected density increases with height. On the contrary, the density due to thermal expansion decreases with height because the upper temperature is higher. As a result, the direction of solutal flow (dashed-line) is just the opposite of the thermal one. However, the key for reversing the radial segregation is to reverse the flow near the interface. For the thermal and solutal convection in Fig. 7a, they can be suppressed by rotation. On the contrary, the solutal convection in Fig. 7b is enhanced by rotation. Therefore, to reduce the solutal effect, higher thermal gradient or lower solute concentration (or lower growth rate) is required. On the other hand, if the solute was heavier than SCN, we anticipate that rotation could be more effective because the flow directions of the double-diffusive flows in Fig. 7 become the same. In other words, the critical rotation speed to reverse the radial segregation can be reduced.

Finally, as illustrated above, for a concave interface there is a critical rotation speed corresponding to the magic-g level, at which the convection is weakest and the solute transport is closer to the diffusion-limited regime (with the largest k_{eff}). In addition to reducing radial solute segregation, near this critical rotation rate we should be able to have a large k_{eff} value for reducing the axial segregation if the growth distance is long enough. Meanwhile, radial segregation could be reduced as well. Furthermore, because local solute accumulation or pit formation can be avoided, morphological instability can be suppressed. Since the rotational field is axisymmetric, rotation dominated convection and solute transport are axisymmetric. High-speed rotation should be useful for reducing asymmetry due to nonuniform heating or ampoule tilting. An interesting application may be in the crystal growth under microgravity, where the unsteady residual gravity or the so-called g-jitter effect prevails. Through 3D time-dependent simulation, Lan and Tu [9] have also illustrated the effectiveness of rotation about the growth axis. Due to the much lower gravity level in space, slow rotation should adequate.

Conclusions

We have built a transparent rotational solidification system to study the effect of rotational field on the solute transport and morphological instability. The solidification of the purified sample was free of constitutional supercooling, so that the microscopically planar interface was possible. To study the solutal effect and morphological instability, a small amount of acetone was injected into the sample. Without rotation, typical pit formation and morphological instability due to double-diffusive convection were illustrated. At medium rotation rate, due to the weakened flow, acetone accumulated quickly near the solidification front leading to an earlier onset of morphological instability. At high rotation rate, the flow direction near the freezing interface was reversed. As a result, acetone accumulated more near the ampoule wall. Overall acetone accumulation near the interface was also reduced. Computer simulation was further carried out to illustrate the observations and good agreement was found. In addition to a deeper insight in the double-diffusive convection and interface morphology, this work provides a simple approach for better

control of solute segregation (both radial and axial) and interface morphology by using rotation. In principle, ampoule rotation in a near axisymmetric thermal environment should have a similar effect.

References

[1] R.J. Schaefer and S. R. Coriell, *Metall. Trans.*, 1984, vol. **15A**, pp. 2109-2115.

[2] C.W. Lan and C.Y. Tu, *J. Crystal Growth*, 2000, vol. **220**, pp. 619-630.

[3] C.W. Lan and C.Y. Tu, *J. Crystal Growth*, 2001, vol. **226**, pp. 406-418.

[4] C.W. Lan, *J. Crystal Growth*, 2001, vol. **229**, pp. 595-600.

[5] C.W. Lan, Y.W. Yang, and C.Y. Tu, *J. Crystal Growth*, 2002, vol. **235**, pp. 619-625.

[6] C.W. Lan and M.C. Liang, *J. Crystal Growth*, 1998, vol. **186**, pp. 203-213.

[7] C.W. Lan, H.Z. Chen, and I.F. Lee, Modeling of double-diffusive flow and morphological instability during vertical Bridgman crystal growth in a rotational field, *J. Crystal Growth*, submitted.

[8] P.M. Adornato and R.A. Brown, *J. Crystal Growth*, 1987, vol. **80**, pp. 155-190.

[9] C.W. Lan and C.Y. Tu, *J. Crystal Growth*, in press.

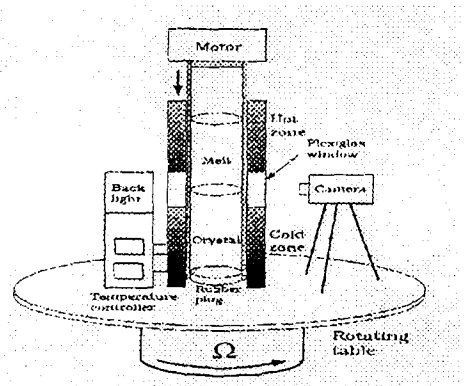

Fig. 1 Schematic of rotational directional solidification

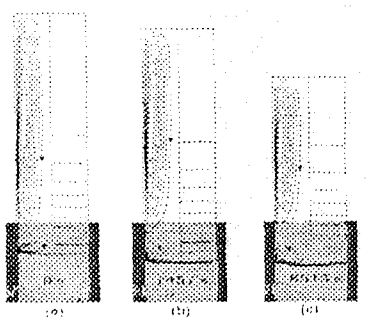

Fig. 2 Observed interface evolution and calculated flow and thermal fields for pure SCN: (a) 0s; (b) 1457s; (c) 8513s after ampoule movement; ampoule pulling speed = 2μm/s. The minimum (Ψ_{min}) and maximum (Ψ_{max}) stream functions are $-1.8\text{x}10^{-4}$ (upper cell) and $2.973\text{x}10^{-5}$g/s in (a), $-1.42\text{x}10^{-4}$ and $3.55\text{x}10^{-4}$g/s in (b), and $-1.387\text{x}10^{-4}$ and $3.73\text{x}10^{-4}$g/s in (c). The spacing for isotherms is $(T_H\text{-}T_m)/10$, where T_H= 353K is the hot zone temperature and T_m= 331.233K the melting temperature of pure SCN.

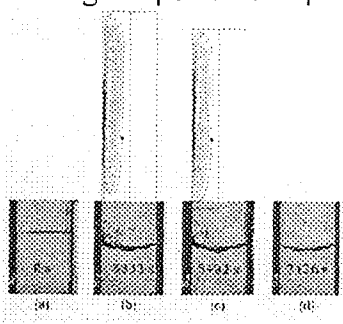

Fig. 3 Observed interface evolution and calculated flow and solute fields for SCN containing 0.007wt% of acetone: (a) 0s; (b) 3833s; (c) 5492s; (d) 7126s after ampoule translation; ampoule pulling speed = 2.5μm/s. Ψ_{min}= $-1.32\text{x}10^{-4}$, Ψ_{max}= 4.498 $\text{x}10^{-4}$g/s, and C_{max}/C_0= 25.4 for (b) and Ψ_{min}= $-1.314\ \text{x}10^{-4}$, Ψ_{max}= 4.448 $\text{x}10^{-4}$g/s, and C_{max}/C_0= 38.961 for (c).

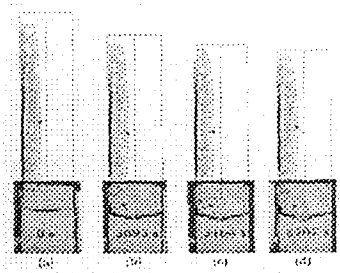

Fig. 4 Observed interface evolution and calculated flow and solute fields for SCN containing 0.007wt% of acetone at 100 RPM rotation: (a) 0s; (b) 3899s; (c) 5164s; (d) 6207s after ampoule translation; ampoule pulling speed = 2.0 μm/s. Ψ_{min}= $-2.224\text{x}10^{-4}$, Ψ_{max}=0 g/s, and C_{max}/C_0= 1 for (a), Ψ_{min}= $-1.82\text{x}10^{-4}$, Ψ_{max}= 1.2 $\text{x}10^{-4}$g/s, and C_{max}/C_0= 30.82 for (b), Ψ_{min}= $-1.817\text{x}10^{-4}$, Ψ_{max}= 1.206 $\text{x}10^{-4}$g/s,

and C_{max}/C_0= 47.5 for (c), and Ψ_{min}= -1.812 x10^{-4}, Ψ_{max}= 1.205 x10^{-4}g/s, and C_{max}/C_0= 66.912 for (d).

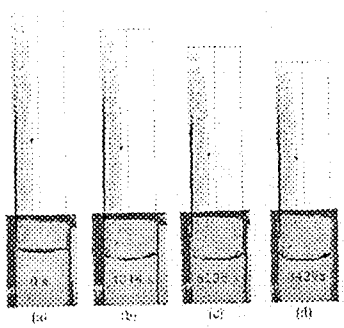

Fig. 5 Observed interface evolution and calculated flow and solute fields for SCN containing 0.007wt% of acetone at 150 RPM rotation: (a) 0s; (b) 4014s; (c) 56195s; (d) 8429s after ampoule translation; ampoule pulling speed = 2μm/s. Ψ_{min}= -2.849x10^{-4}, Ψ_{max}=0 g/s, and C_{max}/C_0= 1 for (a), Ψ_{min}= -2.401x10^{-4}, Ψ_{max}= 2.00 x10^{-5}g/s, and C_{max}/C_0= 9.942 for (b), Ψ_{min}= -2.387x10^{-4}, Ψ_{max}= 2.135 x10^{-5}g/s, and C_{max}/C_0= 12.693 for (c), and Ψ_{min}= -2.365x10^{-4}, Ψ_{max}= 2.18 x10^{-5}g/s, and C_{max}/C_0= 14.384 for (d).

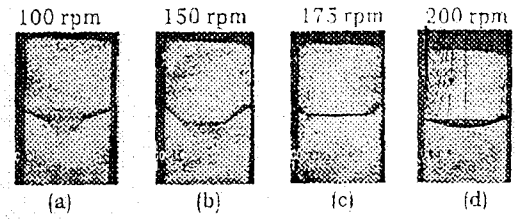

Fig. 6 Effect of rotation rate on the interface shape after 3 hrs of ampoule translation: (a) 100 RPM; (b) 150 RPM; (c) 175 RPM; (d) 200 RPM; ampoule translation = 2.5μm/s. The calculated flow and solute patterns for (d) are also shown, where Ψ_{min}= 2.771x10^{-4}g/s, Ψ_{max}= 4x10^{-7}g/s, and C_{max}/C_0= 6.051.

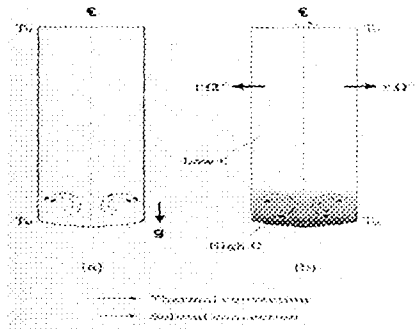

Fig. 7 Illustrated double-diffusive flows due to (a) gravitational; (b) centrifugal acceleration; thermal convection is illustrated by the solid line and the solutal convection by the dashed-line